

**KERNFORSCHUNGSZENTRUM
KARLSRUHE**

Oktober 1967

KFK 633
SM 101/13
EUR 3677 e

Institut für Angewandte Reaktorphysik

Heterogeneity Calculations Including Space Dependent
Resonance Self-Shielding

D. Wintzer



GESELLSCHAFT FÜR KERNFORSCHUNG M. B. H.

KARLSRUHE

Als Manuskript vervielfältigt

Für diesen Bericht behalten wir uns alle Rechte vor

Gesellschaft für Kernforschung m.b.H.

Karlsruhe

KERNFORSCHUNGSZENTRUM KARLSRUHE

Oktober 1967

KFK 633
SM 101/13
EUR 3677 e

Institut für Angewandte Reaktorphysik

HETEROGENEITY CALCULATIONS INCLUDING SPACE DEPENDENT
RESONANCE SELF SHIELDING*

D. Wintzer

Paper to be presented at the IAEA Symposium
on Fast Reactor Physics and Related Safety Problems
held at Karlsruhe, Germany, Oct. 30 - Nov. 3, 1967

Gesellschaft für Kernforschung mbH., Karlsruhe

Work performed within the association in the field of fast reactors
between the European Atomic Energy Community and Gesellschaft für
Kernforschung mbH., Karlsruhe

1. INTRODUCTION

Heterogeneity effects must be taken into account in the interpretation of nearly all experiments performed in the lattices of fast assemblies. Several methods have been developed to calculate the influence of heterogeneity on reactivity, and they work rather well for assemblies with hard spectra.

In fast assemblies with rather soft spectra as in steam cooled fast reactors, the heterogeneity effects in the keV- and 100 eV-region make an important contribution to the heterogeneity effect. In multi-group calculations the modifications of resonance self shielding compared to the homogeneous case must be taken into account. This is done frequently by applying equivalence theorems for effective cross sections, which are based on rational approximations for collision probabilities in the lattice cell. In most applications for fast reactors, Bell's /1/ approximation for tight lattices is used.

However, this procedure is not useful, if the lattice cell contains a material with large resonance cross sections (for example ^{238}U) in more than one region of the cell or if one wants to subdivide a cell region with resonance cross sections in order to investigate the spatial fine structure of reaction rates.

In section 4 of this paper, an approximation is proposed, which takes into account space dependent self shielding in a multiregion lattice cell. The method is based on a multigroup collision probability formalism of reaction rates and neutron emission densities in the cell regions (described shortly in section 2 and 3) and is applied in a computer program called ZERA. The method is not restricted to small heterogeneity effects and can be applied to thermal reactor problems.

The heterogeneity effect on reactivity is often considerably influenced by a modification of leakage parameters due to heterogeneity. In the mentioned program such modifications are roughly taken into account as described in section 6.

Several results of ZERA calculations for rod lattices and for plane lattices are shown in the last section. Some of them are compared with experimental results.

2. BASIC EQUATIONS

We start with the integral form of Boltzmann's equation for the critical reactor. Assuming the reactor to consist of N homogeneous regions, and the fission and scattering processes to be isotropic, we get for the mean flux in region n

$$\phi_n(u) = \sum_{m=1}^N q_m(u) V_m \frac{P_{mn}(u)}{\Sigma_n(u) V_n}. \quad (1)$$

Here Σ and V are symbols for total cross section and volume. The collision probabilities P_{mn} have their usual meaning: the probabilities for neutrons, which are isotropically emitted in region m with spatially constant density to suffer their next collision in region n . So eq. (1) involves the assumption, that the space dependence of the emission density $q(u, \mathcal{r})$ within a region can be neglected. If necessary, a subdivision of regions must be performed.

$q_m(u)$ is the average value of $q(u, \mathcal{r})$ within region m and consists of a fission term (multiplied with an eigenvalue λ) and a downscattering term:

$$q_m(u) = \int_0^{\infty} du' \phi_m(u') \left[\lambda \nu(u' \rightarrow u) \Sigma_{f,m}(u') + \Sigma_{s,m}(u' \rightarrow u) \right] \quad (2)$$

$\Sigma_{f,m}$ is the macroscopic fission cross section in region m , $\Sigma_{s,m}(u' \rightarrow u)$ is the scattering cross section for lethargy transitions from u' to u .

Combining (1) and (2), one gets

$$q_n(u) = \sum_{m=1}^N \frac{V_m}{V_n} \int_0^{\infty} du' q_m(u') \frac{\lambda \nu(u' \rightarrow u) \Sigma_{f,n}(u') + \Sigma_{s,n}(u' \rightarrow u)}{\Sigma_n(u')} P_{mn}(u') \quad (3)$$

The reaction rate for any collision type α (for example capture) in region n is given by

$$F_{\alpha,n}(u) = \Sigma_{\alpha,n}(u) \phi_n(u) V_n = \sum_{m=1}^N V_m q_m \frac{\Sigma_{\alpha,n}(u)}{\Sigma_n(u)} P_{mn}(u) \quad (4)$$

If the reactor or a part of it consists of a periodic lattice, and if the cell concept can be used¹⁾ to calculate the distribution of reaction rates within a unit cell, eqs. (3) and (4) are applicable without formal changes. Only the meaning of two symbols has to be modified: N becomes the number of regions or zones within the unit cell, and the collision probabilities P_{mn} must now include contributions of homological zones in neighbouring cells.

3. MULTIGROUP PRESENTATION

For practical calculations, it is appropriate to use the multigroup approximation and to express the balance equations in terms of group and zone averaged emission densities $q_{g,n}$, fluxes ϕ_{gn} , and reaction rates $F_{g,\alpha,n}$. The corresponding steps in treating eqs. (1) to (4) are integrations which lead to

$$\phi_{g,n} = \sum_{m=1}^N \frac{V_m}{V_n} \left\langle q_m \frac{P_{mn}}{\sum_n} \right\rangle_g \Delta u_g, \quad (5)$$

$$F_{g,\alpha,n} = \sum_{m=1}^N V_m \left\langle q_m \frac{\sum_{\alpha,n} P_{mn}}{\sum_n} \right\rangle_g \Delta u_g, \quad (6)$$

and

$$q_{g,n} = \left\langle q_n(u) \right\rangle_g \Delta u_g = \sum_{m=1}^N \frac{V_m}{V_n} \sum_{k=1}^G \left\langle q_m \frac{\lambda \chi_g \nu \sum_{f,n} + \sum_{k \rightarrow g,n}}{\sum_n} P_{mn} \right\rangle_k \Delta u_k \quad (7)$$

In these equations, the brackets indicate that the average over the energy group g with a lethargy width Δu_g should be taken:

¹⁾ The cell concept is applicable, if the dimensions of the reactor or the lattice zone in question are large compared to the characteristic cell dimension and to the mean free paths of the neutrons.

$$\langle f(u) \rangle_g = \frac{1}{\Delta u_g} \int_{\Delta u_g} f(u) du$$

χ_g is the fraction of fission neutrons born into energy group g , so that

$$\chi_g \cdot \nu(u) = \int_{\Delta u_g} \nu(u \rightarrow u') du'$$

The transfer cross section $\Sigma_{k \rightarrow g, n}$ is defined as

$$\Sigma_{k \rightarrow g, n}(u) = \int_{\Delta u_g} \Sigma_{s, n}(u \rightarrow u') du'$$

G is the number of energy groups.

After separation of the emission density in its average group value $\langle q_m(u) \rangle_g$ and an only weakly²⁾ lethargy dependent function $W_g(u)$ which is normalized to $\langle W(u) \rangle = 1$, eqs. (5) to (7) can be read as

$$\phi_{g, n} = \sum_{m=1}^N \frac{V_m}{V_n} q_{g, m} \langle W(u) \Psi_{mn}(u) \rangle_g \quad (8)$$

$$F_{g, \alpha, n} = \sum_{m=1}^N V_m q_{g, m} \langle W(u) \Sigma_{\alpha, n}(u) \Psi_{mn}(u) \rangle \quad (9)$$

$$q_{g, n} = \sum_{m=1}^N \frac{V_m}{V_n} \sum_{k=1}^G q_{k, m} \langle W(u) [\lambda \chi_g \nu(u) \Sigma_{f, n}(u) + \Sigma_{k \rightarrow g, n}(u)] \Psi_{mn}(u) \rangle_k \quad (10)$$

In these equations the abbreviation

$$\Psi_{mn}(u) = P_{mn}(u) / \Sigma_n(u) \quad (11)$$

has been introduced. $\Psi_{mn}(u)$ is proportional to the flux at lethargy u in region n , caused per unit emission rate in region m .

²⁾ In the sense of the narrow resonance approximation

If the values of the brackets are known, the system of linear equations (10) can be solved to obtain λ , the matrix $q_{g,n}$, group fluxes $\phi_{g,n}$, and reaction rates $F_{g,\alpha,n}$.

The problem is the calculation of the brackets, if the cross sections are strongly energy dependent within the energy group. They appear in the general form

$$A_{g,\alpha,m,n} = \left\langle (u) \sum_{\alpha,n} (u) \psi_{mn}(u) \right\rangle_g \quad (12)$$

and have the physical meaning of a reaction rate in group g and region n caused per unit emission rate in group g and region m . We will call them "reaction coefficients". The bracket in eq. (8) can be regarded as a special case of (12), with $\sum_{\alpha,n} (u) = 1$ and will be denoted as $A_{g,\phi,mn}$.

In principle, it is possible to calculate the collision probabilities and $P_{mn}(u)$ for a series of lethargy points within each energy group and to evaluate the reaction coefficients by numerical integrations. However, if large resonance cross sections must be taken into account this procedure is extremely time consuming and causes difficult computer storage problems.

In order to cope with similar difficulties for homogeneous problems, the Obninsk /2/ group has proposed to use tabulated self-shielding factors for microscopic cross sections. These are defined as

$$f_{\alpha,\nu}(\sigma_{\nu 0}) = \frac{\overline{\sigma_{\alpha,\nu}}}{\langle \sigma_{\alpha,\nu}(u) \rangle} = \frac{1}{\langle \sigma_{\alpha,\nu}(u) \rangle} \frac{\left\langle w(u) \frac{\sigma_{\alpha,\nu}(u)}{\sigma_{\nu}(u) + \sigma_{\nu 0}} \right\rangle}{\left\langle w(u) \frac{1}{\sigma_{\nu}(u) + \sigma_{\nu 0}} \right\rangle} \quad (13)$$

and will be used in the next section.

$\sigma_{\nu 0}$, the background cross section, is the sum of the cross section contributions of other nuclides per atom of nuclide ν ; it is assumed to be constant within the energy group under consideration.

4. CALCULATION OF THE REACTION COEFFICIENTS

Splitting up $A_{g,\alpha,m,n}$ into contributions of individual nuclides

$$A_{g,\alpha,m,n} = \sum_{\nu} A_{g,\nu,\alpha,m,n} \quad (14)$$

leads to

$$A_{g,\nu,\alpha,m,n} = N_{\nu n} \langle w(u) \sigma_{\alpha,\nu}(u) \Psi_{mn}(u) \rangle_g \quad (15)$$

If $\sigma_{\alpha,\nu}(u)$ contains large resonances in group g , the main contributions to $A_{g,\nu,\alpha,m,n}$ will be due to reactions near resonance energies. For this reason, $\Psi_{mn}(u)$ must be carefully calculated near the resonances of nuclide ν . If an overlapping of large resonances of different nuclides does not occur in the cell regions, the energy dependence of Ψ_{mn} at resonance values of σ_{ν} is predominantly determined by the energy dependence of $\sigma_{\nu}(u)$.

If the resonance character of the cross sections must be taken into account in one region n of the cell only, the dependence of Ψ_{mn} on σ_{ν} can be approximated by a rational function (see, for example, /1/ and /3/),

$$\Psi_{m,n}(\sigma_{\nu}(u)) = \frac{a_{\nu,m,n}}{\sigma_{\nu}(u) + b_{\nu}} \quad (16)$$

which is proportional to the fine structure of the spectrum near resonances of σ_{ν} in a fictitious homogeneous medium, as characterized by a background cross section b_{ν} per atom of nuclide ν . The fictitious cross section b_{ν} involves geometrical parameters of the resonance region. The formal agreement of eq. (16) with the resonance behaviour of the flux in a homogeneous medium³⁾ is the substance of the well known equivalence theorem /3/ and makes possible the use of self-shielding factors or resonance integrals in many heterogeneous cases.

3) The formal agreement can be seen by specializing eq. (11) to a one-region cell, which describes a part of a large homogeneous medium with a total cross section $\Sigma(u)$. The collision probability matrix reduces to one number $P_{11} = 1$, and Ψ_{11} becomes

$$\Psi_{11} = \frac{1}{\Sigma(u)} = \frac{1/N_{\nu}}{\sigma_{\nu}(u) + \sigma_{\nu 0}}$$

N_{ν} is the number of atoms of nuclide ν in the medium, $\sigma_{\nu 0}$ the background cross section due to other nuclides.

However, the known equivalence theorems cannot be used in more general cases, in which resonance cross sections of the same nuclide (for example ^{238}U) are present in more than one region of the cell. For this reason, using equivalence theorems, it is not possible to subdivide a region with resonance cross sections, which sometimes would be valuable for studying the spatial fine structure of resonance reactions or to describe more accurately the emission density distribution.

Furthermore, the derivation of (16) is based on a rational approximation for collision probabilities, which is rather inaccurate for plane cells.

Actually, exact functions or good approximations for the dependence of the collision probabilities on cross sections and geometrical parameters are known for most cases of practical interest, but in general they lead to a more complicated function for $\Psi_{mn}(\sigma_\nu)$ than (16).

The main advantages of the equivalence theorems (the separation of reaction coefficients or effective cross sections into nuclide contributions and the use of tabulated self-shielding factors or resonance integrals) can be saved if it is possible to approximate $\Psi_{mn}(\sigma_\nu)$ by series of rational functions, i.e., if

$$\Psi_{mn}(\sigma_\nu) = \sum_{j=1}^J \frac{a_{\nu,j,m,n}}{\sigma_\nu + b_{\nu j}} . \quad (17)$$

Introducing (17) into (15), one gets

$$A_{\nu,\alpha,m,n} = N_{\nu n} \sum_{j=1}^J a_{\nu,j,m,n} \left\langle w(u) \frac{\sigma_{\alpha,\nu}(u)}{\sigma_\nu(u) + b_{\nu j}} \right\rangle . \quad (18)$$

(We have dropped now the group index g .)

The brackets in the last equation can be calculated from self-shielding factors using the relation

$$\left\langle (u) \frac{\sigma_{\alpha,\nu}(u)}{\sigma_\nu(u) + \sigma_{\nu 0}} \right\rangle = \frac{\overline{\sigma_{\alpha,\nu}}}{\overline{\sigma_\nu} + \sigma_{\nu 0}} , \quad (19)$$

which follows from

$$\frac{1}{\left\langle \frac{w(u)}{\sigma_\nu(u) + \sigma_{\nu 0}} \right\rangle} = \overline{\sigma_\nu} + \sigma_{\nu 0}$$

(see eq. (13)).

Similarly as in (16), the parameters $b_{\nu j}$ can be interpreted as background cross sections, which characterize the dilutions of nuclide ν in a set of J fictitious media. Eq. (17) describes a superposition of the corresponding spectra.

In some cases, it is possible to derive reasonable values for $b_{\nu j}$ from physical considerations, in which the special neutron optical parameters of the cell are taken into account. However, it is difficult to do this generally.

For this reason, we do not try to derive the $b_{\nu j}$ from cell parameters, but choose them to make the expression (17) flexible in the cross section interval of interest (that is approximately the interval between $\sigma_{p\nu}$ and the largest resonance cross section $\sigma_{\nu, \max}$ in the energy group).

It was found, that the expression (17) yields a good approximation for the function in the interval $\sigma_{p\nu} < \sigma_{\nu} < \sigma_{\nu, \max}$, if the parameters $b_{\nu j}$ cover about the same interval uniformly on a \log_{10} -scale. The achievable accuracy grows with the number J of terms in (17) (see below).

The coefficients $a_{\nu, j, m, n}$ can be obtained by calculating some values of the function $\Psi_{mn}(\sigma_{\nu}) = P_{mn}(\sigma_{\nu}) / \Sigma_n$ and by fitting the expression (17) to these values.

The advantage of the described approximation is, that it is not restricted to a rational approximation for $P_{mn}(\sigma_{\nu})$. One is free to use exact formulas or the best known approximations for the calculation of collision probabilities and is not limited to a certain type of cell geometry. The methods for P_{mn} -calculations used in the code ZERA for rod lattices and for plane lattices are described in a paper to be published in the near future.

For the investigation of relatively small heterogeneity effects as they occur in fast reactors, the accuracy of the described method can be improved by a slight modification. The approximation (17) is not used for $\Psi_{mn}(\sigma_{\nu})$ but for

$$\Psi_{mn}^*(\sigma_{\nu}) = \Psi_{mn}(\sigma_{\nu}) - \Psi_{mn, \text{hom}}, \quad (18)$$

$$\text{where } \Psi_{mn, \text{hom}} = P_{mn, \text{hom}} / \Sigma_n \quad (19)$$

is the limit of Ψ_{mn} for cells with extremely small dimensions, but with the same compositions and relative region dimensions as the heterogeneous cell. For this limit, the collision probabilities clearly become:

$$P_{m,n,hom} = \frac{\sum_n V_n}{\sum_{m=1}^N \sum_m V_m} \tag{20}$$

At energies near resonances of nuclide ν , $\Psi_{mn,hom}(\sigma_\nu)$ is then

$$\Psi_{m,n,hom} = \frac{1}{\sum_{m=1}^N N_{\nu m} V_m / V_n} \left[\sigma_\nu + \sum_{\nu' \neq \nu} \sigma_{\nu'} \frac{\sum_{m=1}^N N_{\nu' m} V_m}{\sum_{m=1}^N N_{\nu m} V_m} \right] \tag{21}$$

Again, the energy dependence of the second term in the denominator of (21) at resonance values of σ_ν is neglected.

The advantage of approximating $\Psi_{mn}^*(\sigma_\nu)$ instead of $\Psi_{mn}(\sigma_\nu)$ is obvious: for cell dimensions which are small compared to the mean free paths of neutrons a small difference of similar functions is approximated; it is this difference which actually represents the heterogeneity effect.

This modification has been applied in a series of test calculations, and it was found, that a number of approximately 5 terms in (17) is sufficient to get a good approximation for $\Psi_{mn}(\sigma_\nu)$ and to obtain (from eq. (18)) rather accurate reaction coefficients.

Some typical results are shown in Fig. 1 for a two region plate cell which is specified in Table I.

Table I:

| plate number | ²³⁵ U-density | ²³⁸ U-density | H-density | thickness |
|--------------|--------------------------|--------------------------|----------------------|-----------|
| 1 | 1 x 10 ²² | 2 x 10 ²² | - | 1 cm |
| 2 | - | 4 x 10 ²² | 1 x 10 ²² | 1 cm |

The calculations have been performed with cross sections of group 19 of the ABN-set /2/. In this energy group, the resonance self-shielding effects, especially for ^{238}U , are rather strong. (Self-shielding factors vary between 0.023 and 1.) Two of the calculated reaction coefficients, the coefficients for absorption ($A_{a,1,2}$) and elastic scattering ($A_{e,1,2}$) are plotted in Fig. 1a as function of J for constant values $b_{\nu,J} = 400 \sigma_{p\nu}$. The other values $b_{\nu,j}$ were placed equidistantially on a logarithmic σ -scale, with the smallest value $b_{\nu 1} = \sigma_{p\nu}$. The same numbers have been used for the σ_{ν} -values for which the fitting values of ψ_{mn}^* were calculated from (11).

For five or more fictive homogeneous mixtures, the results for $A_{a,1,2}$ do not differ by more than 0.5%, for $A_{e,1,2}$ the agreement is even better.

Fig. 1b shows the dependence of the reaction coefficients on the highest dilution parameter $b_{\nu J}$ (which is also the highest scanning point for $\psi_{mn}^*(\sigma_{\nu})$). All the results shown in Fig. 1b were obtained with 10 fictitious dilutions, so that a good approximation of $\psi_{mn}^*(\sigma_{\nu})$ in the interval $\sigma_{p\nu} < \sigma_{\nu} < \sigma_{\nu J}$ can be assumed. Perhaps it is surprising⁴⁾ that already for $\sigma_{\nu,J} = 400 \sigma_{p\nu}$ rather good results are achieved. However, this may be explained by the fact that in large resonances most of the reactions occur in the flanks.

5. LEAKAGE CORRECTIONS

In order to find a realistic equilibrium spectrum which takes into account the finite size of the lattice, DB^2 -corrections are applied in the cell code ZERA: all reaction rates within an energy group are reduced by a factor

⁴⁾ For ^{238}U , $\sigma_{\nu J} = 400 \sigma_{p\nu} \approx 4000 \text{ b}$ is much smaller than the maximum cross section in group 19 ($\approx 40.000 \text{ b}$).

$$f_B = \frac{\text{removal rate}}{\text{removal rate} + \bar{D}B^2 \sum_{n=1}^N \phi_n V_n} \quad (22)$$

The application of this factor for all cell regions implies the assumption, that the spatial distribution of reaction rates is not influenced by the global diffusion of neutrons.

The group diffusion coefficients \bar{D} are calculated from Benoist's /4/ formula:

$$3\bar{D} \sum_{n=1}^N \phi_n = \sum_{n=1}^N \phi_n V_n \sum_{m=1}^N P_{n,m} / \sum_{tr,m} \quad (23)$$

This formula can be applied, if the Buckling components in the fundamental directions are equal, i.e., if

$$B_x^2 = B_y^2 = B_z^2 = B^2/3 \quad (24)$$

or, for a cylindrical reactor, if

$$B_r^2 = 2B_z^2 = \frac{2}{3} B^2 \quad (24a)$$

If (24) or (24a) do not hold, the anisotropy of diffusion, which is due to streaming effects, must be taken into account. We have not done this, because it demands the complicated calculation of modified collision probabilities (see /4/).

However, we think that (23) at least leads to a reasonable estimate of heterogeneity effects on leakage.

6. DERIVATION AND APPLICATION OF HETEROGENEITY-CORRECTED CROSS SECTIONS

As already mentioned, the solution of eq. (10) leads to the eigenvalue λ and to group- and region-dependent fluxes and reaction rates. $1/\lambda$ is the multiplication factor k_∞ for the infinite lattice, if no buckling corrections are applied. If $\bar{D}B^2$ -corrections are performed as described in the preceding section, $1/\lambda$ becomes the (static) effective multiplication factor k_{eff} for an unreflected finite lattice with a geometrical buckling B^2 . (For a homogeneous one-region cell, λ agrees with the result of zero-dimensional calculations using the same cross section set and the same buckling.)

However, differences in k_{eff} -values of homogeneous and heterogeneous cells do not contain enough information for calculating heterogeneity effects on reactivity for reactors with different lattices in different zones.

For this reason, the code ZERA was extended to calculate "heterogeneity-corrected" cross sections Σ_{α}^* in order to use them in multigroup diffusion codes.

They are derived from

$$\Sigma_{\alpha}^* \cdot \sum_{n=1}^N \phi_n V_n = \sum_{n=1}^N F_{\alpha,n} \quad (25)$$

The transport cross sections are calculated from

$$\Sigma_{\text{tr}}^* = \frac{1}{3\bar{D}} \quad (26)$$

where \bar{D} is given by eq. (23).

It should be mentioned, that these cross sections are nearly independent of the buckling used.

They also can be applied in perturbation codes, if one is interested in the space dependence of heterogeneity effects. In this case the reactor which is being perturbed is calculated with cross sections corresponding to homogeneous cells.

In fast reactors with rod lattices, the heterogeneity effect on the diffusion coefficients and the anisotropy of diffusion are usually rather small. Both become more important for reactors with plate lattices, because of the large free paths of neutrons, which impinge under a small angle to the plate surface into plates with small cross sections. The fraction of neutrons, which have large paths in a cell region with small cross sections is for geometrical reasons appreciably larger than in an equivalent rod lattice cell with the same volume fractions of the cell regions.

If the cell thickness of a plate lattice is small compared to the mean free path of neutrons perpendicular to the plate surfaces, it can be expected, that the diffusion coefficient D_z corresponding to a flux gradient perpendicular to the plates is hardly influenced by heterogeneity.

Eq. (23) gives the mean of the diffusion coefficients for the three fundamental directions:

$$\bar{D} = (\bar{D}_x + \bar{D}_y + \bar{D}_z)/3 \quad (27)$$

Since in the homogeneous case it is

$$D_{\text{hom}} = D_x = D_y = D_z \quad , \quad (28)$$

the difference between \bar{D} and D_{hom} is

$$\bar{D} - D_{\text{hom}} = \frac{1}{3} \left[(\bar{D}_x - D_{\text{hom}}) + (\bar{D}_y - D_{\text{hom}}) + (\bar{D}_z - D_{\text{hom}}) \right] . \quad (29)$$

If the thickness of a plate cell is small enough to neglect $\bar{D}_z - D_{\text{hom}}$, and if we consider a cylindrical reactor, eq. (29) reduces to:

$$\bar{D} - D_{\text{hom}} = \frac{2}{3} (\bar{D}_r - D_{\text{hom}}) \quad (30)$$

or

$$\bar{D}_r - D_{\text{hom}} = \frac{3}{2} (\bar{D} - D_{\text{hom}}) \quad (30a)$$

$$\bar{D}_z - D_{\text{hom}} = 0 . \quad (30b)$$

7. APPLICATIONS

The heterogeneity experiments performed in SNEAK, Assembly 3A-1, were analyzed using the methods described above. The radial dependence of reactivity changes due to bunching, together with calculated curves, is plotted in Fig. 2b. A short description of the experiments is presented in /5/. Fig. 2a contains the structure of the normal and bunched cells.

The calculated curves (solid lines in Fig. 2b) were gained with a perturbation code by using heterogeneity corrected group cross sections as described in section 6. The heterogeneity corrections for the diffusion coefficients were calculated from (30a) and (30b). The agreement between experiment and calculation is satisfactory near the core center. Only a qualitative agreement is achieved near the core boundary.

The dashed lines in Fig. 2b do not contain any heterogeneity corrections for the diffusion coefficients. They can not explain the change in sign of the bunching effect in the boundary region of the core.

Figures 3 and 4 give some insight into the energy distribution of the heterogeneity effects in a central core zone, in which the spectrum can be assumed to be the equilibrium spectrum corresponding to an energy independent buckling. The curves shown are based on ZERA calculations, in which the buckling has been iterated to give $k_{eff} = 1$. Fig. 3 shows the relative difference between the heterogeneous and homogeneous spectrum, calculated as $\Delta\phi_{g,n}/\phi_g(hom) = (\phi_{g,n}(het) - \phi_g(hom))/\phi_g(hom)$. The spectra are normalized to the same number of fission neutrons per unit time and volume. The solid lines correspond to the uranium plates, the circles to the steel CH_2 plates. The values of the two remaining other plates in the cell generally lie between the uranium and the steel CH_2 points. The flux concentration in the uranium plates in the MeV-region is the reason for the main contribution to the bunching effect on reactivity (compare Fig. 4). The spatial flux distribution in this energy region seems to be rather well calculated, as can be concluded from a comparison of Rh-activation distributions with calculated values (see /5/). Enlarged diffusion and diminished CH_2 -downscattering upon bunching in the MeV-region lead to a lower flux in all cell regions in the 100 keV region. This is the reason for the negative reactivity contributions in Fig. 4. Below 10 keV, the emission density peaks in the polyethylene; and the flux depression in the uranium lead to a remarkable softening of the spectrum (in all plates) in the low energy region, which causes reactivity gains.

It can be seen from Fig. 4, that the heterogeneity effects are a result of partially compensating positive and negative effects. The compensating character and the complicated energy distribution tend to make the total reactivity effect rather sensitive to changes in the cross sections used. This is an explanation for the appreciable difference between the results gained with the ABN- and the SNEAK-set (see Fig. 2a).

It should be noted, that the mean hydrogen concentration (7.37×10^{20} atoms/cm³) is much lower than in a high pressure steam cooled reactor, which will be simulated in SNEAK-3A-2. The contributions

from the energy region below 10 keV to the total reactivity effect will be considerably larger in SNEAK-3A-2.

Heterogeneity effects in the low energy region are of major importance for the reactivity behaviour during flooding of a steam cooled fast reactor. Fig. 5 gives an impression of the magnitude of the effects for the reference reactor D1, which is described in /6/. In this figure, the results of cell calculations for the effective multiplication factor k_{eff} for both the homogeneous and the heterogeneous case are plotted vs. steam density. The curve for the homogenized core was gained by reducing all cell dimensions by a factor 10^3 . The buckling was chosen to give $k_{\text{eff}} \approx 1$ at the normal steam density (0.07 g/cm^3). The results show that the calculations for the homogenized core lead to errors of several percent in k_{eff} at high steam densities.

An application of the described method to a cell of a hexagonal light-water moderated lattice of a thermal reactor is shown in Fig. 6, which shows the calculated distribution of ^{238}U -captures within a natural uranium rod in the energy region from 3 eV to 10 keV. The rod diameter is 0.983 cm, the rod center-to-center spacing 1.44 cm. The measured curve and the results of Monte Carlo calculations are taken from /7/. The calculated capture densities and the measured curve are normalized to 1 in the center of the rod. The ZERA-calculations have been performed with ABN cross section. In order to find the space dependence of the reaction rates within the rod, the rod was subdivided into 12 concentric regions.

This application is a rather sensitive test for the reaction coefficients, which account for the spatial dependence of resonance self shielding. The agreement with the experimental curve and with the results of Monte Carlo calculations is surprisingly good. This holds also for the total number of neutrons absorbed in the energy region under consideration in ^{238}U per neutron entering at 10 keV: ZERA gives a number of 0.3140, while the Monte Carlo result is 0.3075.

8. SUMMARY AND CONCLUSIONS

The described method to deal with resonance self shielding in multi-region lattice cells in principle reduces the calculation of resonance reactions to the calculation of collision probabilities for some values of the resonance cross sections. It is applicable to a wide range of cell problems, because it is not restricted to the use of rational approximations for the collision probabilities.

The method is used in a FORTRAN-program ZERA which calculates group and region dependent reaction rates, k_{eff} -values for unreflected lattices, and heterogeneity corrected cross sections, which can be used to calculate heterogeneity effects in different regions of a reactor.

The ZERA results are in good or satisfactory agreement with the bunching effects on reactivity, which were measured in SNEAK-3A-1. The results show the importance of the leakage component of heterogeneity effects in the outer regions of a reactor. The heterogeneity corrections to the diffusion coefficients allow an estimate of this component. The agreement between predicted and experimental results in a core boundary region in SNEAK-3A-1 is not yet satisfactory. Further investigations are planned in this direction.

In fast reactors containing hydrogen, the energy dependence of heterogeneity effects on reaction rates is rather complicated and has a surprisingly strong dependence on the cross sections used. For this reason, the investigation of heterogeneity effects also can be helpful for testing cross section sets.

9. ACKNOWLEDGEMENTS

I wish to thank Prof. W. Häfele and Dr. P. Engelmann for their encouragement of this work and for very valuable discussions. Thanks are also due to Mr. G. Bruhn for his help with the difficult programming work.

References

- /1/ G.I. Bell: "A Simple Treatment for Effective Resonance Cross-Sections in Dense Lattices" Nucl. Sci. Eng. 5, 138 (1959)

- /2/ L.P. Abagjan et al.: "Gruppenkonstanten schneller und intermediärer Neutronen für die Berechnung von Kernreaktoren" KFK-tr-144 (Translation)

- /3/ L. Dresner: "Resonance Absorption in Nuclear Reactors" Pergamon Press (1960)

- /4/ P. Benoist: "Théorie du coefficient de diffusion des neutrons dans un réseau comportant des cavités" CEA-R-2278 (1964)

- /5/ D. Stegemann et al.: "Physics Investigations of a 670 l Steam Cooled Fast Reactor System in SNEAK, Assembly 3A-1". This conference.

- /6/ A. Müller et al.: "Referenzstudie für den 1000 MWe dampfgekühlten schnellen Brutreaktor (D1)", KFK-392 (1966)

- /7/ G. Smith, J. Hardy, Jr., D. Klein: "Comparison of Measurements with a Monte Carlo Calculated Spatial Distribution of Resonance Neutron Capture in a Uranium Rod", Nucl. Sci. Eng. 8, 449 (1960)

FIG. 1a DEPENDENCE OF REACTION COEFFICIENTS
ON THE NUMBER J OF TERMS IN EQ.(17)

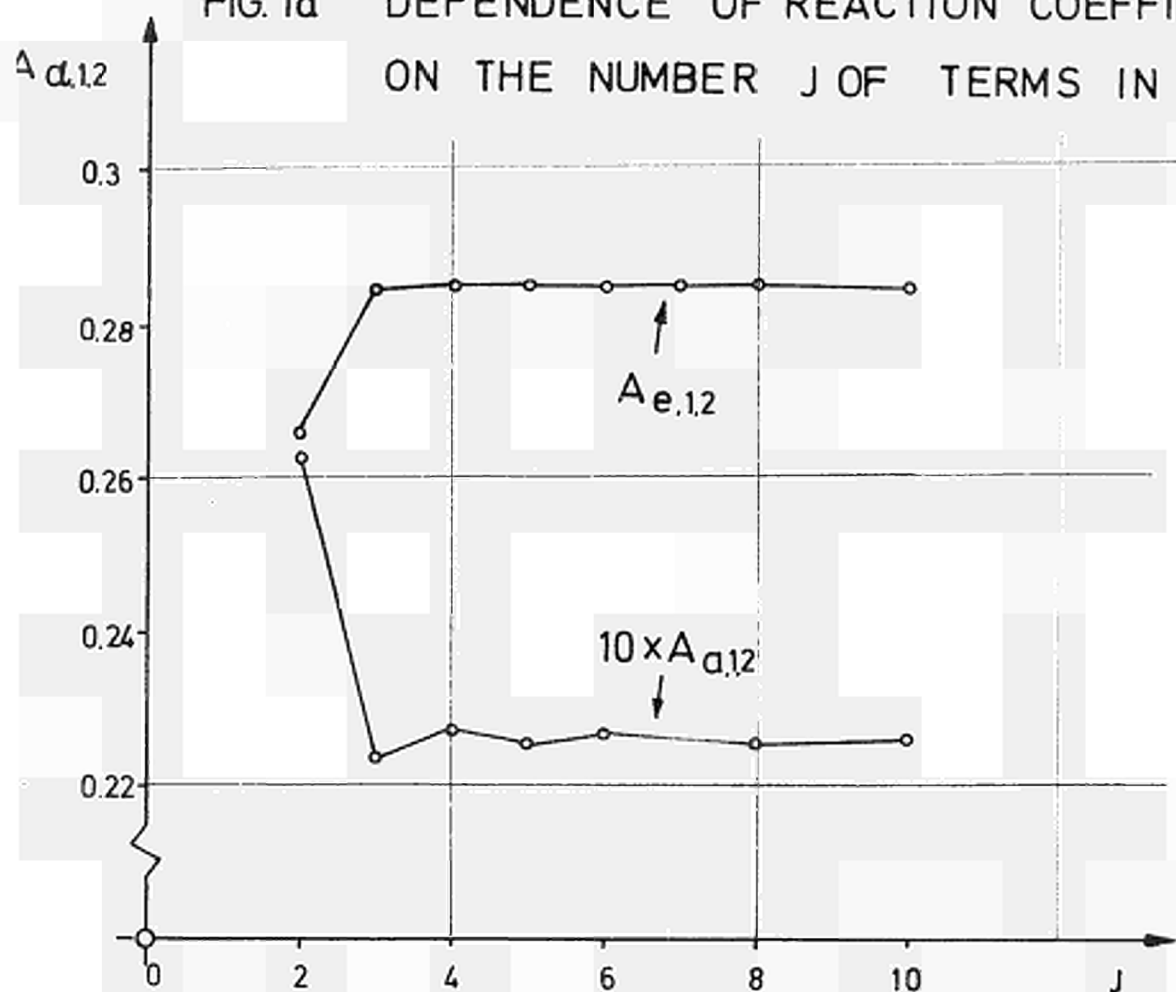
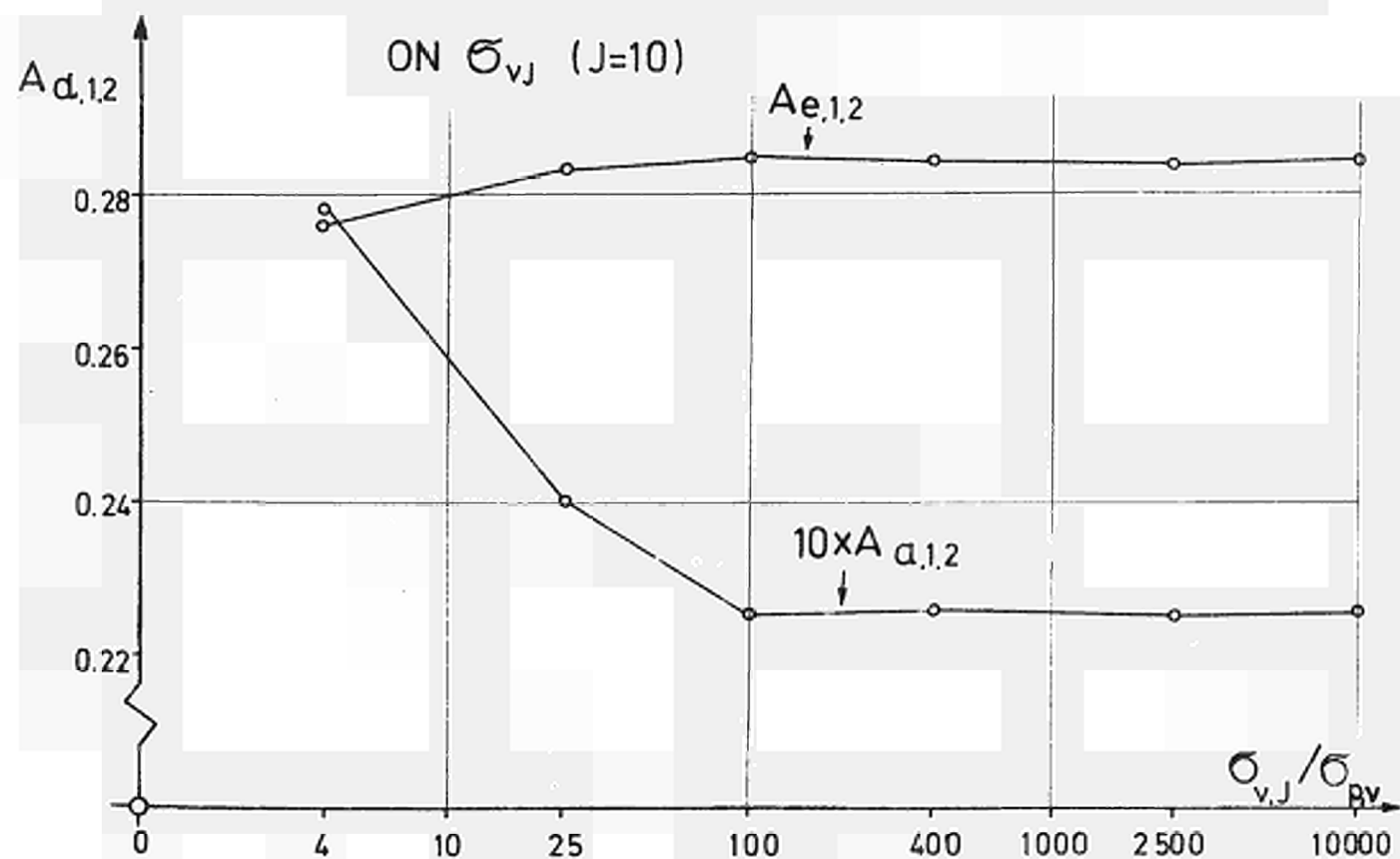


FIG. 1b DEPENDENCE OF REACTION COEFFICIENTS
ON $\sigma_{v,J}$ ($J=10$)



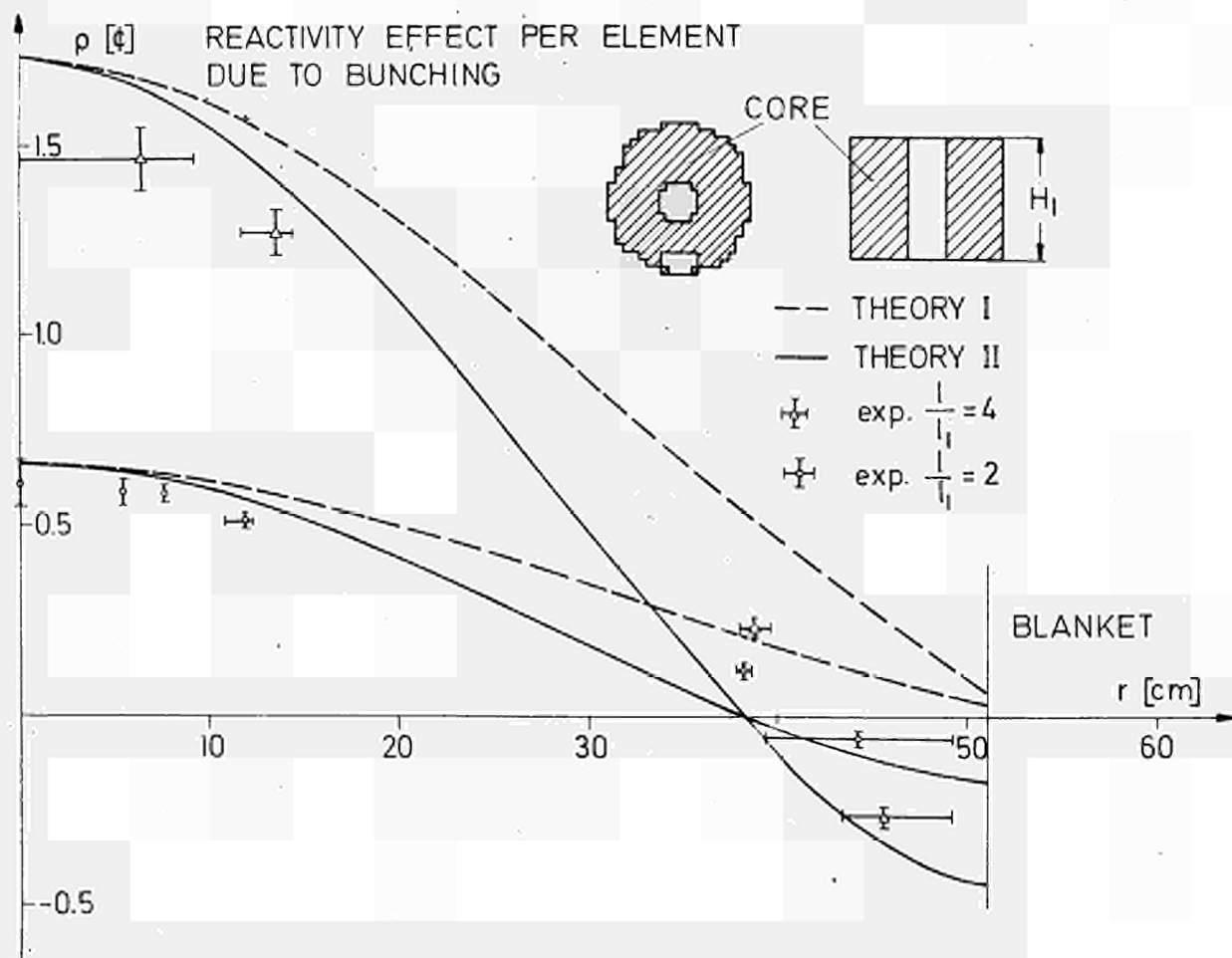
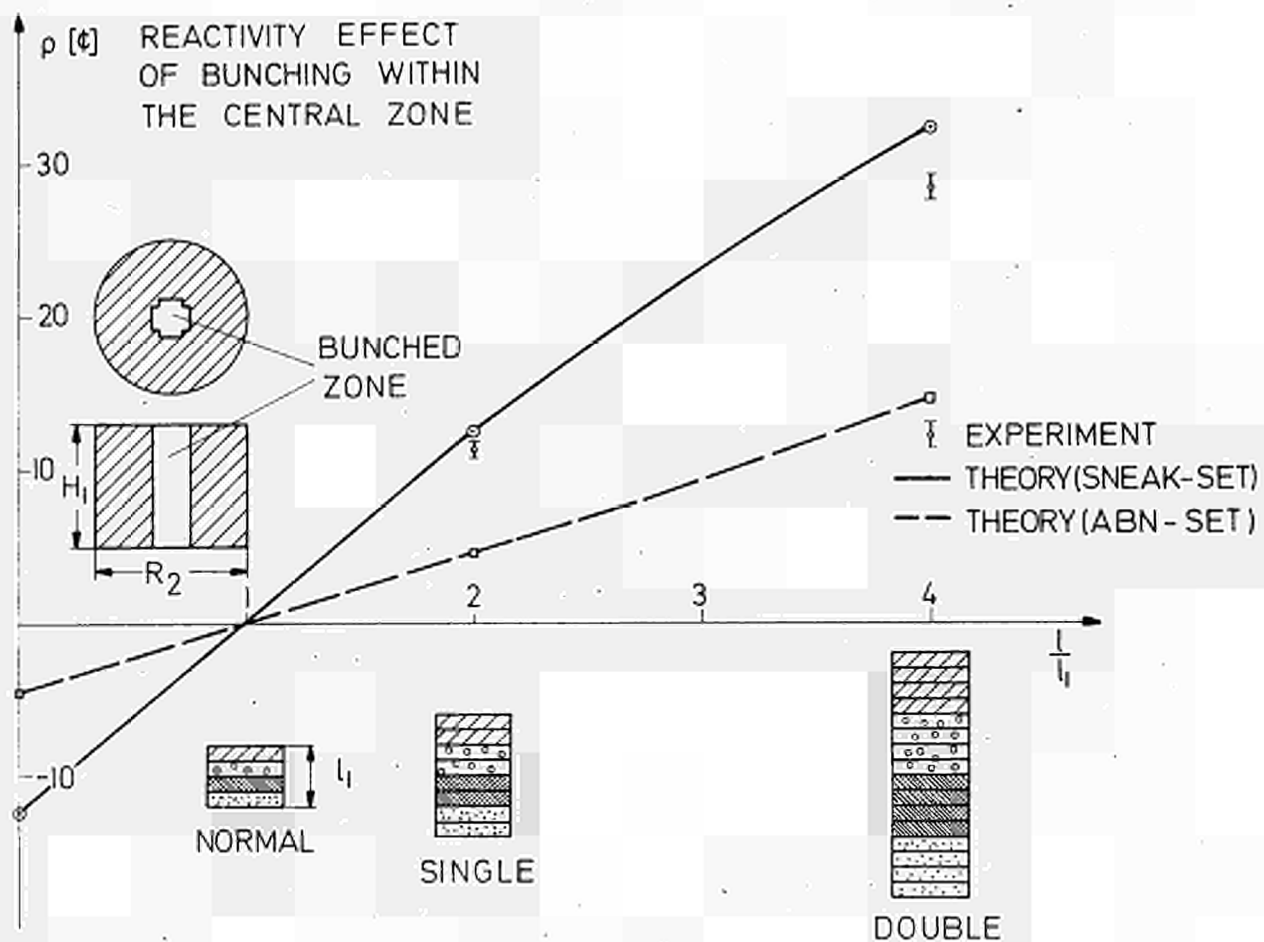


FIG. 2 a,b REACTIVITY EFFECTS OF SINGLE AND DOUBLE BUNCHING IN SNEAK ASSEMBLY 3A-1

FIG. 3 RELATIVE FLUX CHANGES CAUSED BY THE HETEROGENEOUS CELL STRUCTURE IN SNEAK 3A -1

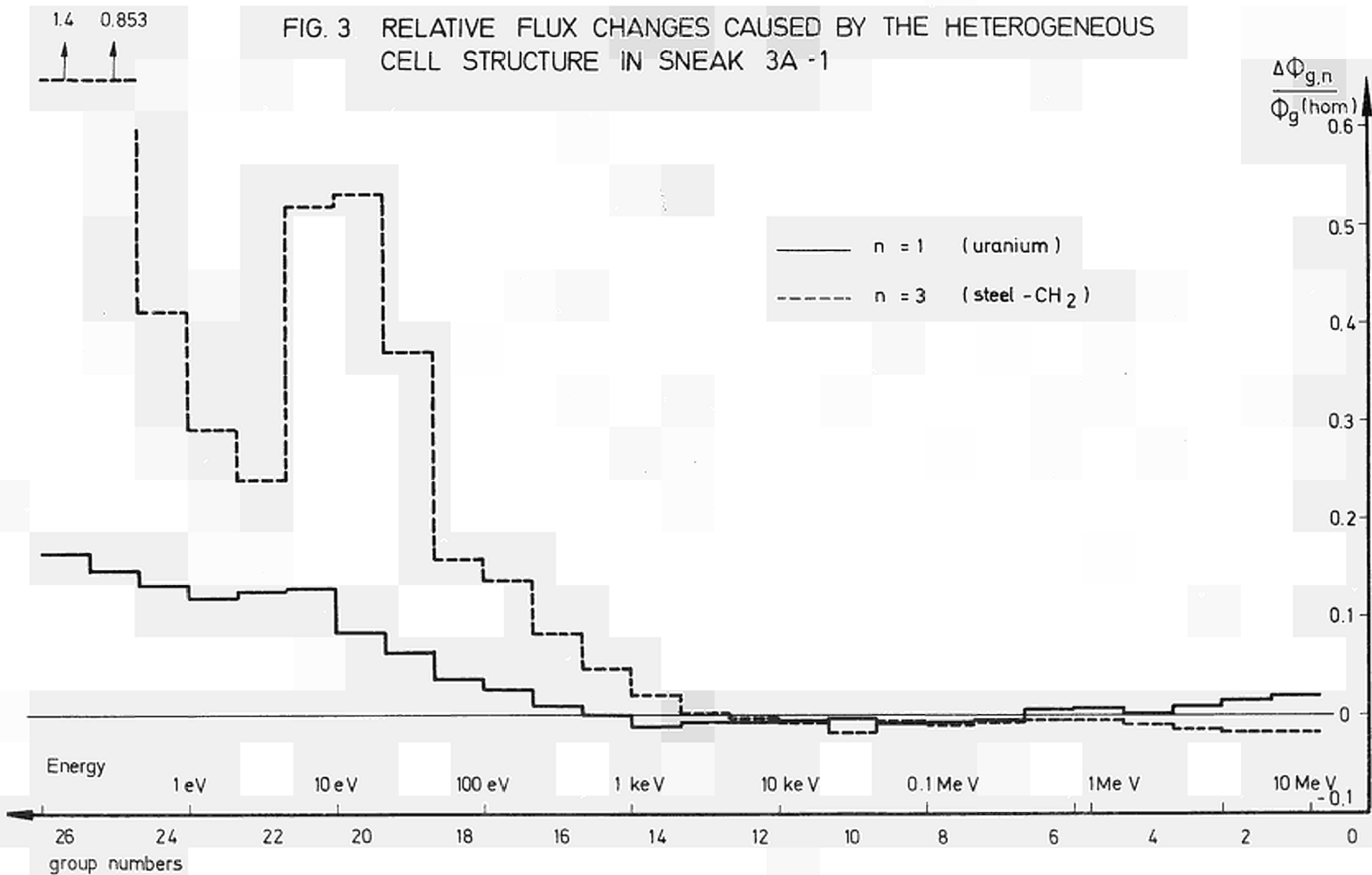


FIG.4 ENERGY DISTRIBUTION OF THE BUNCHING EFFECT ON REACTIVITY IN SNEAK 3A-1

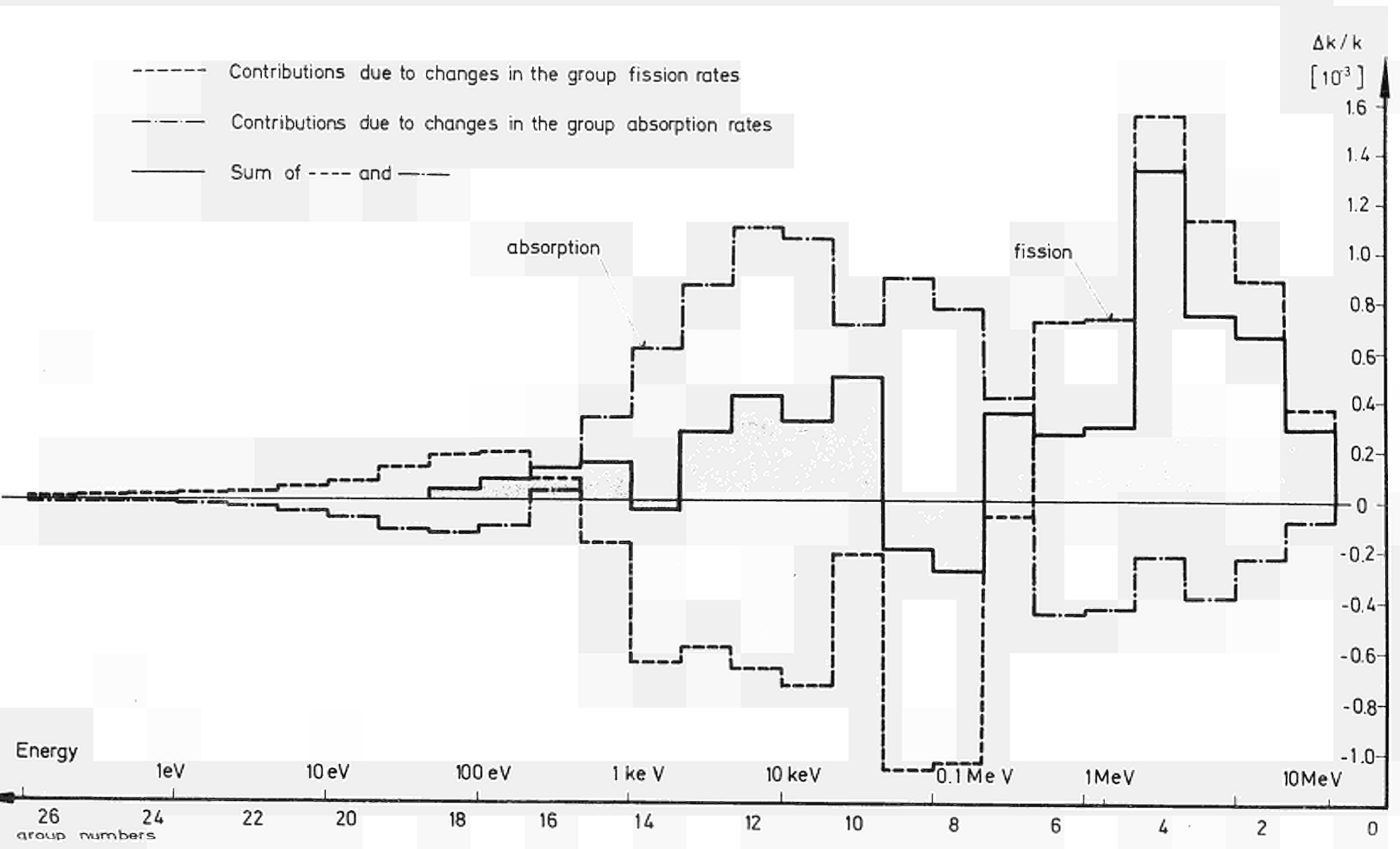


FIG. 5 k_{eff} VS. STEAM DENSITY FOR D1

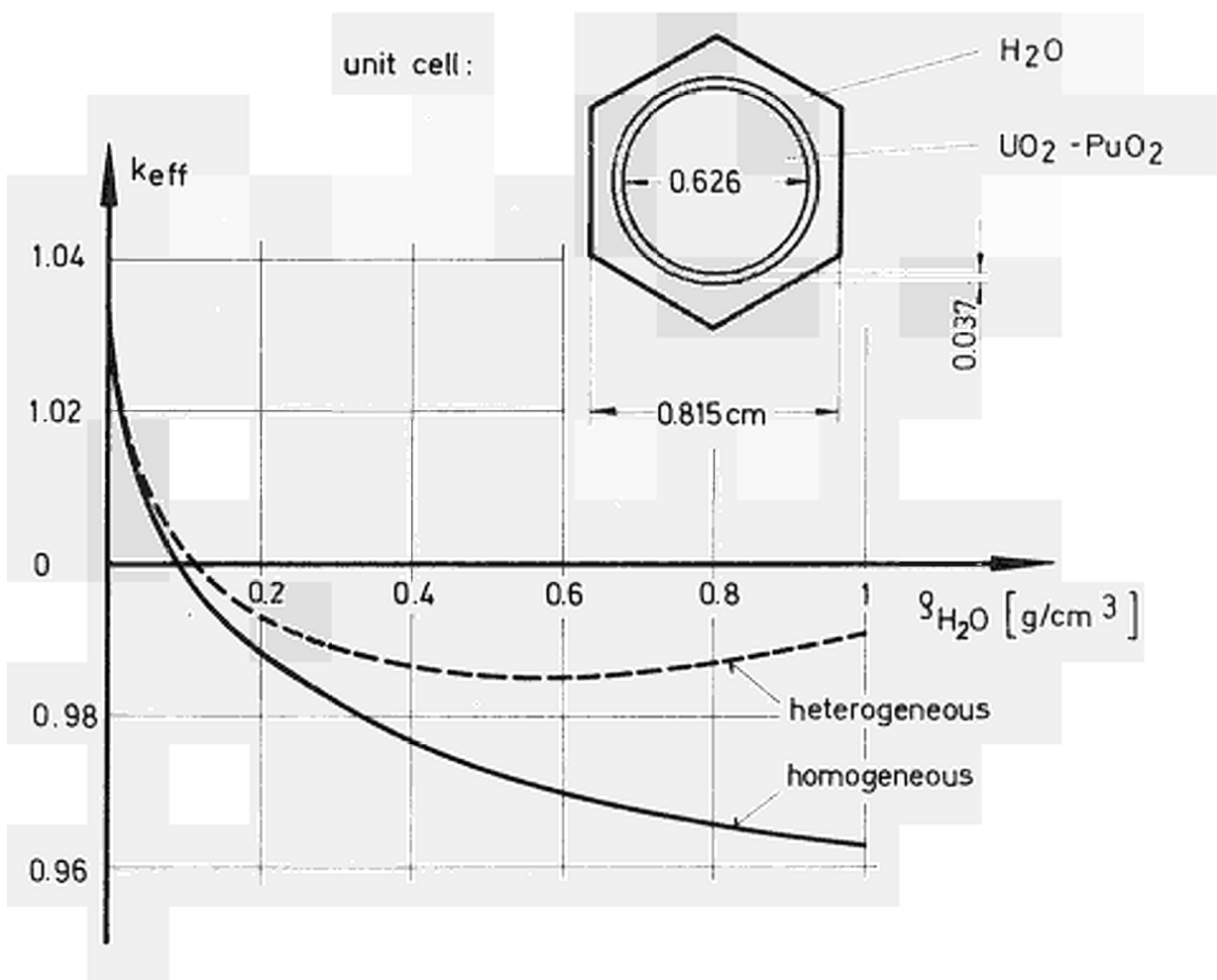
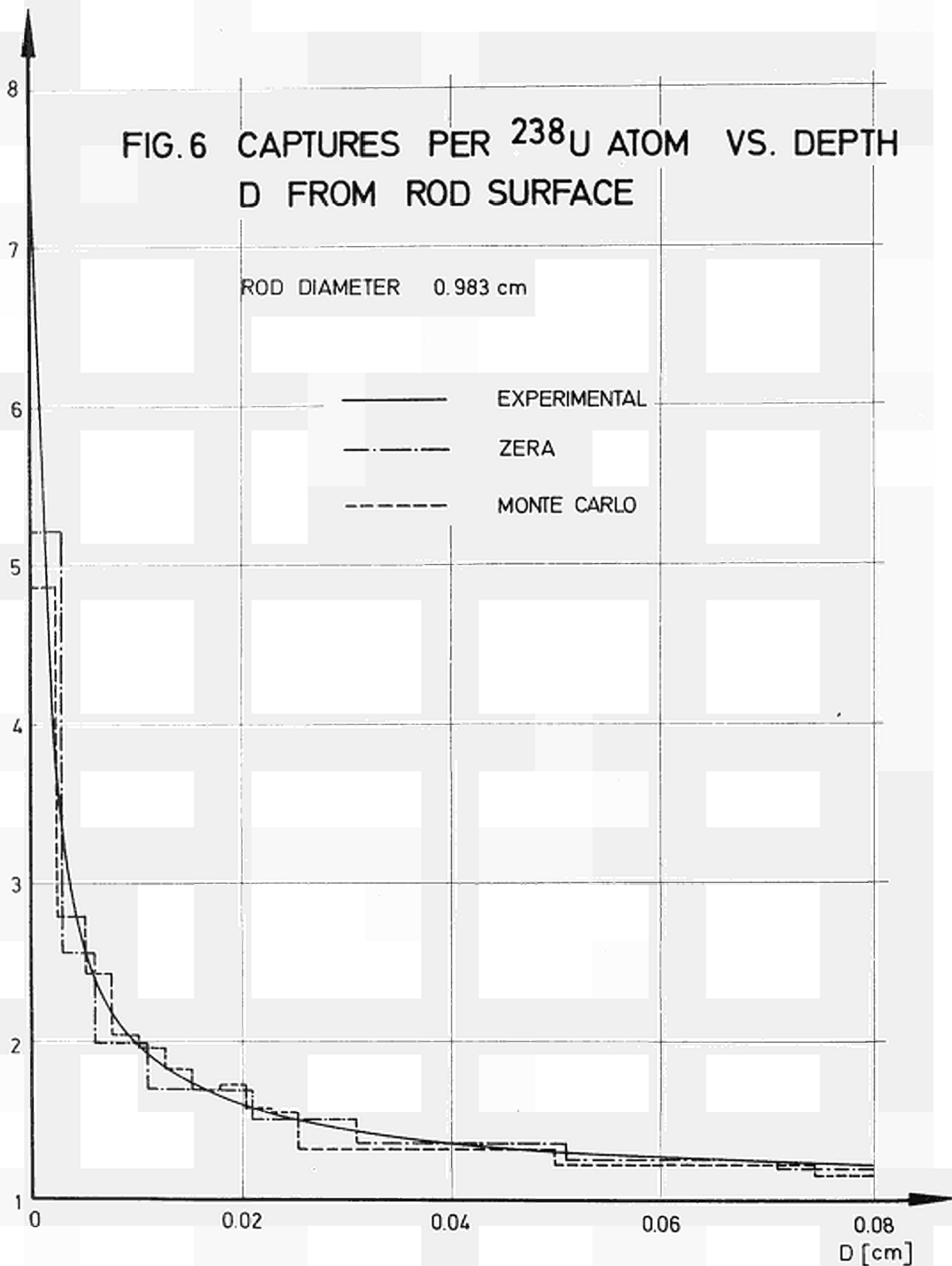


FIG.6 CAPTURES PER ^{238}U ATOM VS. DEPTH
D FROM ROD SURFACE



CDNA03677ENC